Magnetic phase diagrams of Gd-H, Tb-H, Dy-H systems

Victoria Chzhan[1], *Irina* Tereshina [2,*], *Gennady* Burkhanov[1], *Galina* Politova[1] and *Henryk* Drulis[3]

[1]Baikov Institute of Metallurgy and Materials Science RAS, 119334 Moscow, Russia
[2] Lomonosov Moscow State University, Faculty of Physics, 119991 Moscow, Russia
[3]Institute of Low Temperature and Structural Research, 50-422 Wroclaw, Poland

Abstract. We study the impact of hydrogen impurity on the magnetic phase transition temperatures of the high purity rare-earth metals Gd, Tb and Dy. Prior to hydrogenation, the rare earths were purified by the vacuum distillation method. Hydrogenation was carried out using a Sievert-type apparatus. Magnetic phase diagrams were constructed based on the thermomagnetic analysis.

1 Introduction

Characterization of physicochemical properties of the rare earth (R) metals should be performed on purified [1] samples due to their high chemical activity and strong affinity for gas-forming impurities. Literature survey revealed a large number of works dedicated to the description of the *R*'s properties [2-6]. However, electrical and magnetic properties studies were performed on single- and polycrystalline samples of various degrees of purity [7]. This unfortunately disables a direct comparison of the results obtained by different authors. It also makes it difficult to reveal intrinsic physical processes occurring in the metals. It is therefore important to use high-purity metals for the studies. Controlled doping (by e.g. gas-forming impurities) of the previously purified metal allows us to determine the influence of a particular impurity on the properties of a material under study. In this paper, a systematic study of the hydrogenation effect on magnetic properties of a distilled gadolinium, terbium and dysprosium is carried out. (The interest to Gd is due to its high magnetocaloric properties near room temperature that allow its use as a working body in magnetic refrigerators [8-10].) *R*'s interaction with hydrogen is rather extensively studied. Phase diagrams of *R*-H for heavy rare-earth metals and yttrium have common features (see Fig. 1a) [11]. Special attention in this paper is devoted to the study of the impact of hydrogenation on the phase transitions temperatures for small hydrogen concentrations ($x \leq 1.2$).

2 Materials synthesis and experimental details

Rare-earth metals Gd, Tb and Dy were purified by vacuum distillation [1]. High purity rare earths are characterized by a reduced content of gas-forming impurities (10^{-2} -10^{-3} wt. %). The metals purity with respect to the content of ~70 impurity elements are 99.92-99.96 wt. %. The amount of absorbed hydrogen was determined by measuring the pressure change in the reactor chamber after completing the reaction. The accuracy of the hydrogen concentration determination is 0.02 hydrogen atoms per formula unit (at.H/f.u.). The samples for hydrogenation and further studies were cut out of the central portions of the distillate [12]. Appearance of a rare-earth distillate is shown in Fig. 1b.

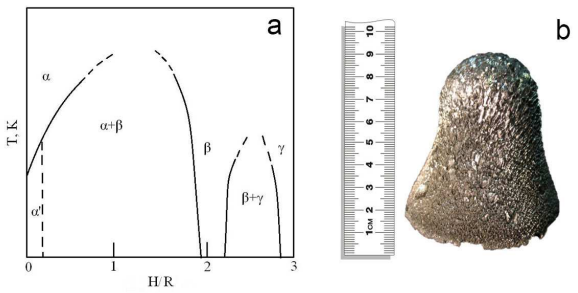

Fig. 1. Typical phase diagram of a hydrogenated rare earth (a) [11]. Appearance of a rare-earth distillate (b).

Purified metals were hydrogenated using a Sievert-type apparatus with hydrogen (impurities content < 10^{-3} – 10^{-4} vol. %) pressures up to 0.1 MPa. The samples of GdH_x (x = 0, 0.02, 0.05, 0.09, 0.12, 0.13, 0.16, 0.2), DyH_x (x = 0, 0.1, 0.2, 0.5, 0.7, 0.9, 1.2) and TbH_x (x = 0, 0.1, 0.2, 0.3, 0.5, 0.7, 0.9, 1.2) were obtained and investigated. Magnetic properties of the samples were studied over wide temperature range using a vibrating sample magnetometer equipped with a step motor [13]. Thermomagnetic analysis was carried out in a magnetic field of 0.02 T in the temperature range 4.2-300 K. The relative accuracy of data acquisition did not exceed 0.5%. The Curie temperatures of the parent and hydrided Gd were also determined by means of the Arrott-Belov plot method based on the thermodynamic theory [14].

* Corresponding author: irina_tereshina@mail.ru

3 Results and discussion

The *R*-H phase diagrams (Fig. 1a) are characterized by a region of existing solid-solutions in the *R* phase (α-RH_x) having the structure of the parent *R*, as well as by the presence of β-RH_2 and γ-RH_3 phases with a variable composition. The β-RH_2 dihydride phase has a *fcc* CaF_2-type lattice and the γ-RH_3 trihydride phase crystallizes into a hexagonal HoH_3-type structure [11,15].

All the parent and hydrogenated samples of Gd, Tb and Dy were investigated by the X-ray diffraction analysis from the surface. The X-ray analysis indicated that a distilled Gd, and all obtained α-GdH_x solid-solutions are single-phase and have an *hcp* structure (space group *P6₃/mcc*) [12,14]. A similar crystalline structure is also present in the distilled Tb and Dy. The obtained structural characteristics are in good agreement with the literature [16]. It was found that all of the TbH_x and DyH_x samples contain two phases. In addition to the main α-RH_x solid-solution phase, a cubic β-RH_2 phase was found. The amount of the second phase increases linearly with the increasing of absorbed hydrogen content. For example, for the sample $DyH_{1.2}$, the amount of β-DyH_2 is 66 %. The Néel temperatures T_N and magnetic moments μ of the RH_2 dihydrides are listed in Table 1.

Table 1. Magnetic characteristics of the RH_2 dihydrides [19].

R	T_N, K	μ, μ_B
Gd	21	6.5
Tb	17	7.4
Dy	3.5	6.4

No data on the possible maximum hydrogen concentration in terbium and dysprosium solid solutions at room temperature is available in literature.

Experimental values of phase transition temperatures can vary depending on the method used for the determination [7]. The use of magnetic field typically leads to higher values of magnetic phase transition temperatures. The application of magnetic fields exceeding critical values for the particular compounds can also lead to the magnetic order change. In this work, the experiments were unified, i.e. we performed our measurements under the same conditions and the samples for the study had the same shape, thus enabling [17] precise determination of the changes in the magnetic state upon hydrogen absorption.

Previously the Curie temperatures of Gd were determined from the Arrott-Belov plots as 291 K [14]. The magnetic phase transition temperatures of the parent distilled Gd, Tb and Dy, and the same samples after hydrogenation were determined by using a thermomagnetic analysis ($\mu_0 H$ = 0.02 T). The critical temperatures were found from the peak of derivative of magnetization dM(T)/dT. Two pronounced extrema were observed on the dM(T)/dT curve in the distilled Gd. The one at T_C = 292 K is associated with the transition from the ferromagnetic (FM) to the paramagnetic (PM) state in the distilled Gd and the other one at T_{SR}=223 K - with a spin-reorientation transition (SRT). According to Ref. 18, during the SRT the magnetic moments of Gd aligned along the *c*-axis at higher temperatures begin to deviate from the *c*-axis. The angle reaches 70º at 170 K, and then it decreases to ~30º at lower temperatures. It was found that α-GdH_x solid solutions below the Curie temperature retain the ferromagnetic properties. Figure 2a shows the temperature dependencies of magnetization for α-$GdH_{0.1}$. In the solid solution α-$GdH_{0.1}$ hydrogenation is found to increase the transition temperatures to T_C = 294 K and T_{SR} = 234 K (see inset into Fig. 2a). Note that introduction of 0.1 H/Gd increases the T_C by 2 K while the T_{SR} is increased by as much as ~ 10 K.

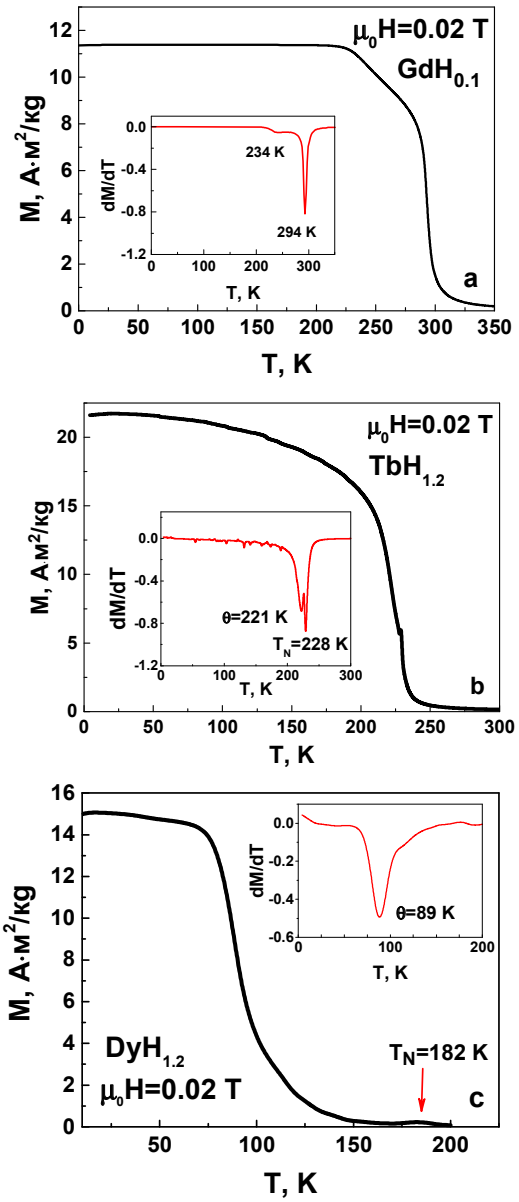

Fig. 2. The temperature dependencies of magnetization for α-$GdH_{0.1}$ (a), $TbH_{1.2}$ (b), $DyH_{1.2}$ (c). Insets show the temperature dependencies of the derivative dM/dT for the mentioned samples.

In contrast to ferromagnetic Gd, Tb and Dy are antiferromagnetic (AFM) below the T_N and have a second transition from the AFM to the FM state at a

temperature θ. In Dy, however, the AFM region exists in a much wider (~90 K) temperature range than that in Tb (~10 K). The presence of the β-TbH_2 and β-DyH_2 antiferromagnetic phase does not have a significant effect on the M(T) dependence behavior because of their low ordering temperatures (see Table 1). As an example, Fig. 2 shows the magnetization curves of $TbH_{1.2}$ (2b) and $DyH_{1.2}$ (2c). As can be seen from the M(T) curves, the sharp decrease in the magnetization occurs at the temperature θ thus implying a change of the magnetic state. At higher temperatures, a maximum observed on the M(T) curves corresponds to the Néel temperature of the samples. Hydrogen addition in Tb and Dy up to the concentration of x = 1.2 H/R does not influence the M(T) behavior. Also two magnetic phase transitions are preserved while the temperatures T_N and θ decrease. Interestingly, similar magnetic behavior with two magnetic phase transitions was also demonstrated by rare-earth-Fe alloys e.g. R_2Fe_{17} (R = Ce [20] and Lu [21]). The temperatures of magnetic phase transitions and the magnetic structures are extremely sensitive to the interstitial impurity atoms (hydrogen, in particular) [22,23], to substitutional atoms [24] and high pressure [25]. The magnetic phase diagrams of such compositions have been obtained and studied extensively in literature [26].

We also constructed magnetic phase diagrams for α-GdH_x, TbH_x, and DyH_x. The effect of hydrogen addition on the T_C's of Gd is demonstrated in Fig. 3. As it is seen from the $T_C(x)$ dependence, the Curie temperature increases by about 5 K when x increases from 0 to 0.2 H/Gd. High pressure experiments give an opposite trend for T_C [27] and therefore the volume effect is very important. The main mechanisms of the Curie temperature increase are discussed in Ref. 15. Figures 4 and 5 show the concentration dependencies of the Néel temperature and the transition temperature from the AFM to the FM state (θ) on the hydrogen content (x) in TbH_x and DyH_x, respectively. Change in the phase transition temperatures is within 1 K in TbH_x when the hydrogen concentration (x) varies from 0 to 1.2 H/Tb. The Néel temperatures of DyH_x decrease from 184 to 182 K, and the temperature θ decreases from 94 to 89 K when x varies between 0 and 1.2 H/Dy. Although the variations in the R phase transition temperatures ranging between 1 and 5 degrees were also recorded previously [28-30], they cannot be attributed to a particular impurity but rather to a mixture of impurities absorbed by a metal. In this study, we were able to identify the real magnetic phase transitions temperatures and their variation as a function of hydrogen impurity content in Gd, Tb and Dy by using parent high purity samples and then those with a controlled impurity composition.

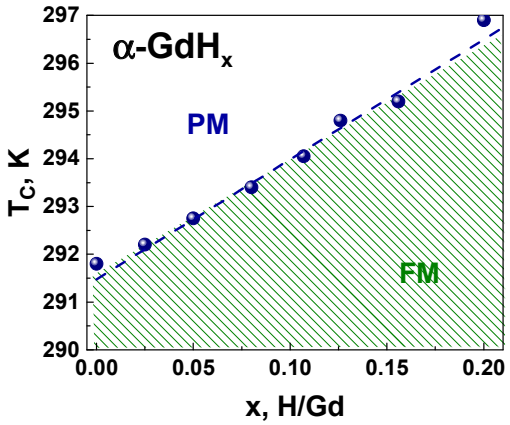

Fig. 3. The Curie temperature T_C *vs.* hydrogen content x in the α-GdH_x solid solutions.

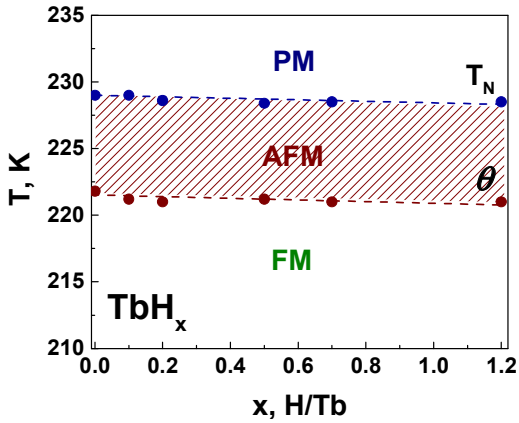

Fig. 4. Concentration dependencies of the Néel temperature T_N and the temperature θ on the hydrogen content x in TbH_x obtained in the magnetic field of 0.02 T.

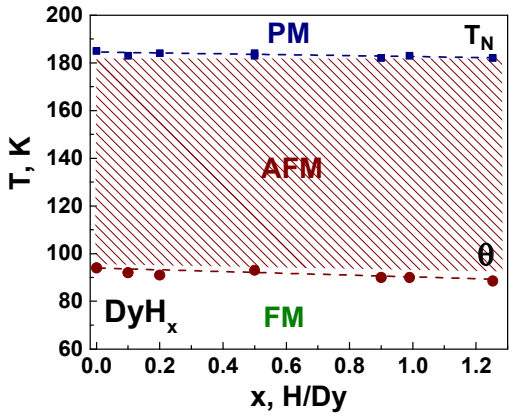

Fig. 5. Concentration dependencies of the Néel temperature T_N and the temperature θ on the hydrogen content x in DyH_x obtained in the magnetic field of 0.02 T.

4 Conclusions

The effect of hydrogenation on the magnetic phase transition temperatures for the three rare earths Gd, Tb, Dy having the highest magnetic ordering temperatures

among *R*s is studied. Gadolinium has a Curie temperature T_C = 292 K. Tb and Dy have complex magnetic structures and display two magnetic phase transitions (FM-AFM and AFM-PM). It is found that hydrogen introduced into the Gd crystal lattice increases the Curie temperature in the range of existence of solid solutions. On the contrary Tb and Dy retain the values of magnetic phase transition temperatures or even have it slightly decreased under the influence of hydrogen. This is due to the presence of the second dihydride phase. As a main achievement, the refined magnetic characteristics of Gd, Tb and Dy after hydrogen treatment are obtained. It is important for the materials working in a hydrogen-containing environment [31].

This work was supported by the Russian Foundation for Basic Research, project no. 16-03-00612-a.

References

1. G.G. Devyatykh, G.S. Burkhanov, *High-Purity Refractory and Rare-Earth Metals* (Cambridge: Int. Sci. Publ., 1997)
2. S.A. Nikitin, *Magnetic Properties of Rare-Earth Metals and Compounds* (Moscow, Publishing House MSU, 1989) (in Russian)
3. V.I. Zverev, A.M. Tishin, A.S. Chernyshov, Ya. Mudryk, K.A. Gschneidner Jr., V.K. Pecharsky, J. Phys.: Condens. Matter **26**, 066001 (2014)
4. A.S. Chernyshov, A.O. Tsokol, A.M. Tishin, K.A. Gschneidner, Jr., V.K. Pecharsky, Phys. Rev. B. **71**, 184410 (2005)
5. M. Mito, K. Matsumoto, Yu. Komorida, H. Deguchi, S. Takagi, T. Tajiri, T. Iwamoto, T. Kawae, M. Tokita, K. Takeda. J. Phys. Chem. Solids **70**, 1290 (2009)
6. D. Michels, C. E. Krill, R. Birringer, J. Magn. Magn. Mater. **250**, 203 (2002)
7. S.Yu. Dan'kov, A.M. Tishin, V.K. Pecharsky, K.A. Gschneidner, Jr., Phys. Rev. B **57**, 3478 (1998)
8. A.M. Aliev, A.B. Batdalov, L.N. Khanov, V.V. Koledov, V.G. Shavrov, I.S. Tereshina, S.V. Taskaev, J. Alloys Compounds **676**, 601 (2016)
9. S.V. Taskaev, M.D. Kuz'min, K.P. Skokov, D.Yu. Karpenkov, A.P. Pellenen, V.D. Buchelnikov, O. Gutfleisch, J. Magn. Magn. Mater. **331**, 33 (2013)
10. Yu.S. Koshkid'ko, J. Cwik, T.I. Ivanova, S.A. Nikitin, M. Miller, K. Rogacki, J. Magn. Magn. Mater. **433**, 234 (2017)
11. P. Vajda, *Handbook on the Physics and Chemistry of Rare Earths* **20**, 207 (Amsterdam: North-Holland, 1995)
12. G.S. Burkhanov, N.B. Kolchugina, E.A. Tereshina, I.S. Tereshina, G.A. Politova, V.B. Chzhan, D. Badurski, O.D. Chistyakov, M. Paukov, H. Drulis, L. Havela, Appl. Phys. Lett. **104**, 242402 (2014)
13. V.I. Nizhankovskii, L.B. Lugansky. Meas. Sci. Technol. **18**, 1533 (2007)
14. E. Tereshina, S. Khmelevskyi, G. Politova, T. Kaminskaya, H. Drulis, I. Tereshina, Sci. Rep. **6**, 22553 (2016)
15. Y. Fukai, *The Metal-Hydrogen System. Basic bulk properties* (Berlin: Springer, 2005)
16. F.H. Spedding, B.J. Beaudry, J. Less Comm. Metals. **25**, 61 (1971)
17. V.I. Zverev, R.R. Gimaev, A.M. Tishin, Ya. Mudryk, K.A. Gschneidner, Jr., V.K. Pecharsky, J. Magn. Magn. Mater. **323**, 2453 (2011).
18. H.E. Nigh, S. Legvold, F. Spedding, Phys. Rev. **132**, 1092 (1963)
19. W.G. Bos, K.H. Gayer, J. Nucl. Mater. **18**, 1 (1966)
20. A.G. Kuchin, N.V. Mushnikov, M.I. Bartashevich, O. Prokhnenko, V.I. Khrabrov, T.P. Lapina, J. Magn. Magn. Mater. **313**, 1 (2007)
21. S.A. Nikitin, I.S. Tereshina, N.Yu. Pankratov, E.A. Tereshina, Yu.V. Skourski, K.P. Skokov, Yu.G. Pastushenkov, Phys. Solid State **43**, 1720 (2001)
22. E.A. Tereshina, A.V. Andreev, J. Kamarád, O. Isnard, J. Appl. Phys. 105, 07A747 (2009)
23. I.S. Tereshina, S.A. Nikitin, K.P. Skokov, T. Palewski, V.V. Zubenko, I.V. Telegina, V.N. Verbetsky, A.A. Salamova, J. Alloys Compounds, **350**, 264 (2003)
24. E.A. Tereshina, O. Isnard, A. Smekhova, A.V. Andreev, A. Rogalev, S. Khmelevskyi, Phys. Rev. B **89**, 094420 (2014)
25. E.A. Tereshina, A.V. Andreev, J. Kamarad, H. Drulis, J. Alloys Compounds **492**, 1 (2010)
26. W. Iwasieczko, A.G. Kuchin, H. Drulis, J. Alloys Compounds **392**, 44 (2005)
27. H. Bartholin, D. Bloch, Phys. Rev. **188**, 845 (1969)
28. G.S. Burkhanov, V.B. Chzhan, G.A. Politova, J. Cwik, N.B. Kolchugina, I.S. Tereshina, Doklady Physics **61**, 168 (2016)
29. F.H. Spedding, J. Less Comm. Metals. **25**, 61 (1971)
30. K.A. Gschneidner, J. Alloys Compd. **193**, 1 (1993)
31. A.P. Kamantsev, V.V. Koledov, V.G. Shavrov, I.S. Tereshina, Solid State Phenomena **215,** 113 (2014)